XLIII CILAMCE
21-25, November, 2022
FOZ DO IGUAÇU - PR - BRAZIL

Geometrically Nonlinear Isogeometric Analysis of Functionally Graded Solids

Elias Saraiva Barroso[1], Evandro Parente Jr.[1], John Williams Ferreira de Souza[1], Marcelo Silva Medeiros Jr.[1], Renan Melo Barros[1].

[1]*Laboratório de Mecânica Computacional e Visualização (LMCV), Departamento de Engenharia Estrutural e Construção Civil, Universidade Federal do Ceará, Campus do Pici, Bloco 728, 60440-900, Fortaleza/CE-Brazil*
elias.barroso@gmail.com, evandro@ufc.br, johnwilliams@alu.ufc.br, marcelomedeiros@ufc.br, renanmelo@alu.ufc.br

Abstract. Functionally Graded Materials (FGM) are composites with a gradual and continuously varying composition. Given the constituents, the volume fraction is evaluated by a mathematical function and the effective properties by a homogenization method. Composite structures made of FGM are commonly analyzed using Finite Elememt Method (FEM). Isogeometric Analysis (IGA) is an alternative to FEM where the displacement field is approximated using the same basis functions employed in geometric representation, as B-Splines or NURBS. This work presents an isogeometric formulation for geometrically nonlinear analysis of functionally graded solids based on trivariate basis functions. Numerical results are evaluated for small and large displacements problems, and excellent results are obtained in all examples and gradations studied. Furthermore, the results showed that using higher order functions leads to faster convergence, requiring fewer degrees of freedom in comparison to lower order functions.

Keywords: Functionally Graded Materials, Isogeometric analysis, Geometric Nonlinearity , 3D analysis

1 Introduction

Functionally Graded Materials (FGM) are composites with a continuously varying composition. Due to this characteristic, they allow a better stress distribution when compared to laminated composites [1]. The effective properties are evaluated by the employment of homogenization methods. Many of these techniques have already been presented in the literature, with the Rule of Mixtures being the most used one, due to its simplicity, and the Mori-Tanaka being a popular alternative, presenting higher similarity with experimental results.

The design of composite structures is commonly performed using a CAE (Computer-Aided Engineering) system, where the modeling step is performed in a CAD (Computer-Aided Design) component and structural analysis is realized using the Finite Element Method (FEM), both integrated into the CAE system. Isogeometric Analysis (IGA) is an alternative to FEM where the displacement field is approximated using the same basis functions employed in geometric representation, as B-Splines and NURBS [2]. Therefore, the model geometry is exact regardless of refinement level and the analysis model can be easily refined using well-known algorithms from the geometric modeling field, as degree elevation and knot insertion.

This work presents an isogeometric formulation for geometrically nonlinear analysis of functionally graded solids using trivariate NURBS to describe not only the geometry and displacement field, but also the volume fraction variation. In this formulation, the material gradation is defined by the volume fractions of the control points. Based on these values, the same basis functions used to describe the geometry and to approximate the displacement field are also used to represent the volume fraction variation within the structure. The composite effective properties are evaluated in terms of the constituents volume fractions in any given point. This idea represents an extension to IGA of the graded finite elements proposed by Paulino and Kim [3].

The proposed formulation can be applied to general functionally graded solids with arbitrary tridirectional volume fraction variations. Due to the use of NURBS basis functions, mesh discretization can be easily carried out using standard algorithms of knot insertion and degree elevation. Numerical results are evaluated for small and large displacements problems, and excellent results are obtained in all examples and gradations studied.

2 Isogeometric Analysis

Isogeometric Analysis (IGA) was first proposed by Hughes et al. [2] as a way to model an exact geometry described by Non-Uniform Rational B-Splines (NURBS). These functions were already vastly employed in Computer Aided Design (CAD), and IGA extends them to Computer Aided Engineering (CAE), where NURBS are also employed to approximate the displacement field. The method can represent exact geometries even using coarse meshes. Furthermore, model refinements are obtained using the geometric modeling algorithms of knot insertion (h-refinement) and degree elevation (p-refinement).

A NURBS solid is defined by a tensor product between trivariate rational bases $R_{ijk,p}(\xi, \eta, \zeta)$ and a tensor of control points $\mathbf{P}_{ijk}$:

$$V(\xi, \eta, \zeta) = \sum_{i=1}^{n_{b1}} \sum_{j=1}^{n_{b2}} \sum_{k=1}^{n_{b3}} R_{ijk,p}(\xi, \eta, \zeta)\, \mathbf{P}_{ijk} \tag{1}$$

n_{b1}, n_{b2} and n_{b3} are the number of basis in each parametric direction, which depends on the NURBS degree and knot vector in each direction. The trivariate rational basis is computed by:

$$R_{ijk,p}(\xi, \eta, \zeta) = \frac{\hat{w}_{ijk}\, N_{i,p}(\xi)\, N_{j,q}(\eta)\, N_{k,l}(\zeta)}{\displaystyle\sum_{\hat{i}=1}^{n_{b1}} \sum_{\hat{j}=1}^{n_{b2}} \sum_{\hat{k}=1}^{n_{b3}} \hat{w}_{\hat{i}\hat{j}\hat{k}}\, N_{\hat{i},p}(\xi)\, N_{\hat{j},q}(\eta)\, N_{\hat{k},l}(\zeta)} \tag{2}$$

where $\hat{w}_{ijk}$ is the control point weight, used to represent rational geometries (e.g. conics and quadrics), and $N_{i,p}(\xi)$, $N_{j,p}(\eta)$ and $N_{k,p}(\zeta)$ are univariate B-spline bases.

Once the Isogeometric analysis is used, the basis functions are first employed to model the geometry:

$$x = \sum_{i=1}^{n} R_i\, x_i, \quad y = \sum_{i=1}^{n} R_i\, y_i, \quad z = \sum_{i=1}^{n} R_i\, z_i \tag{3}$$

where n is the number of control points.

In IGA, the same basis functions are used to approximate the displacement field inside the model:

$$u = \sum_{i=1}^{n} R_i\, u_i, \quad v = \sum_{i=1}^{n} R_i\, v_i, \quad w = \sum_{i=1}^{n} R_i\, w_i \tag{4}$$

where u_i, v_i, and w_i are the displacements corresponding to each control point. Furthermore, in the present formulation, the same basis functions are also used to describe the material gradation:

$$V_c = \sum_{i=1}^{n} R_i\, V_{c_i} \tag{5}$$

where V_{c_i} is the ceramic volume fraction corresponding to each control point.

The effective properties associated to the FG solids varies together with the volume fraction distribution. Utilizing the simplest homogenization technique, the Rule of Mixtures, the effective properties are computed using:

$$P = P_m + (P_c - P_m)\, V_c \tag{6}$$

where P represents the desired property, V is the volume fraction and the subscripts c and m represent the ceramic and metal respectively. The Rule of Mixtures may overestimate the structural stiffness, presenting high discrepancies when compared to experimental data. Thus, many other homogenization techniques (or micromechanical models) have been presented in the literature [4]. It is important to note that the IGA formulation proposed in this work is independent of the adopted homogenization technique.

2.1 Strains and stresses

Since FG composites are formed by the inclusion of small particulate reinforcement, they often present isotropic nonhomogeneous behavior. Thus, constitutive equations are very similar to that of isotropic materials, but with material properties changing along the structure. For 3D models, the constitutive matrix is given by:

$$\boldsymbol{\sigma} = \mathbf{C}\,\boldsymbol{\varepsilon} \Rightarrow \begin{Bmatrix} \sigma_x \\ \sigma_y \\ \sigma_z \\ \tau_{xy} \\ \tau_{xz} \\ \tau_{yz} \end{Bmatrix} = \frac{E}{(1+\nu)(1-2\nu)} \begin{bmatrix} (1-\nu) & \nu & \nu & 0 & 0 & 0 \\ \nu & (1-\nu) & \nu & 0 & 0 & 0 \\ \nu & \nu & (1-\nu) & 0 & 0 & 0 \\ 0 & 0 & 0 & \frac{(1-2\nu)}{2} & 0 & 0 \\ 0 & 0 & 0 & 0 & \frac{(1-2\nu)}{2} & 0 \\ 0 & 0 & 0 & 0 & 0 & \frac{(1-2\nu)}{2} \end{bmatrix} \begin{Bmatrix} \epsilon_x \\ \epsilon_y \\ \epsilon_z \\ \gamma_{xy} \\ \gamma_{xz} \\ \gamma_{yz} \end{Bmatrix} \tag{7}$$

where E and ν are the homogenized Young's modulus and Poisson's ratio, which can be evaluated by Eq. (6).

The strains can be evaluated by:

$$\boldsymbol{\varepsilon} = \boldsymbol{\varepsilon}_0 + \boldsymbol{\varepsilon}_L = \mathbf{H}\,\boldsymbol{\beta} + \frac{1}{2}\mathbf{A}\,\boldsymbol{\beta} \tag{8}$$

where:

$$\boldsymbol{\beta} = \begin{Bmatrix} u_{,x} \\ u_{,y} \\ u_{,z} \\ v_{,x} \\ v_{,y} \\ v_{,z} \\ w_{,x} \\ w_{,y} \\ w_{,z} \end{Bmatrix} = \sum_{i=1}^{n} \begin{bmatrix} R_{i,x} & 0 & 0 \\ R_{i,y} & 0 & 0 \\ R_{i,z} & 0 & 0 \\ 0 & R_{i,x} & 0 \\ 0 & R_{i,y} & 0 \\ 0 & R_{i,z} & 0 \\ 0 & 0 & R_{i,x} \\ 0 & 0 & R_{i,y} \\ 0 & 0 & R_{i,z} \end{bmatrix} \begin{Bmatrix} u_1 \\ v_1 \\ w_1 \\ \vdots \\ u_{n_p} \\ v_{n_p} \\ w_{n_p} \end{Bmatrix} = \mathbf{G}\,\mathbf{u} \tag{9}$$

and

$$\mathbf{H} = \begin{bmatrix} 1 & 0 & 0 & 0 & 0 & 0 & 0 & 0 & 0 \\ 0 & 0 & 0 & 0 & 1 & 0 & 0 & 0 & 0 \\ 0 & 0 & 0 & 0 & 0 & 0 & 0 & 0 & 1 \\ 0 & 1 & 0 & 1 & 0 & 0 & 0 & 0 & 0 \\ 0 & 0 & 1 & 0 & 0 & 1 & 1 & 0 & 0 \\ 0 & 0 & 0 & 0 & 0 & 0 & 0 & 1 & 0 \end{bmatrix} \qquad \mathbf{A} = \begin{bmatrix} u_{,x} & 0 & 0 & v_{,x} & 0 & 0 & w_{,x} & 0 & 0 \\ 0 & u_{,y} & 0 & 0 & v_{,y} & 0 & 0 & w_{,y} & 0 \\ 0 & 0 & u_{,z} & 0 & 0 & v_{,z} & 0 & 0 & w_{,z} \\ u_{,y} & u_{,x} & 0 & v_{,y} & v_{,x} & 0 & w_{,y} & w_{,x} & 0 \\ u_{,z} & 0 & u_{,x} & v_{,z} & 0 & v_{,x} & w_{,z} & 0 & w_{,x} \\ 0 & u_{,z} & u_{,y} & 0 & v_{,z} & v_{,y} & 0 & w_{,z} & w_{,y} \end{bmatrix} \tag{10}$$

Substituting Eq. (9) in Eq. (8):

$$\boldsymbol{\varepsilon} = \mathbf{H}\,\mathbf{G}\,\mathbf{u} + \frac{1}{2}\mathbf{A}\,\mathbf{G}\,\mathbf{u} = \left(\mathbf{B}_0 + \frac{1}{2}\mathbf{B}_L\right)\mathbf{u} = \mathbf{B}\,\mathbf{u} \tag{11}$$

where:

$$\mathbf{B}_0 = \mathbf{H}\,\mathbf{G}, \qquad \mathbf{B}_L = \mathbf{A}\,\mathbf{G} \tag{12}$$

Thus, strains depend on matrix $\mathbf{B}$, which has a linear and a nonlinear term ($\mathbf{B}_0$ and $\mathbf{B}_L$, respectively).

2.2 Equilibrium equations

The static equilibrium equations of the model can be obtained using the virtual work principles:

$$\int_V \delta\varepsilon^T\,\boldsymbol{\sigma}\,dV = \int_V \delta\mathbf{u}^T\,\mathbf{b}\,dV + \int_S \delta\mathbf{u}^T\,\mathbf{q}\,dS \tag{13}$$

where $\delta\mathbf{u}$ is the virtual displacement vector, $\delta\boldsymbol{\varepsilon}$ is the virtual strain vector, and $\boldsymbol{q}$ and $\boldsymbol{b}$ are the surface and body loads, respectively. This equation can be rewritten in terms of the internal (**g**) and external (**f**) forces:

$$\delta\mathbf{u}^T\,\mathbf{g} = \delta\mathbf{u}^T\,\mathbf{f} \quad \Rightarrow \quad \mathbf{g} = \mathbf{f} \tag{14}$$

where:

$$\mathbf{g} = \int_V \overline{\mathbf{B}}^T \boldsymbol{\sigma}\, dV, \qquad \mathbf{f} = \int_V \mathbf{N}^T\,\mathbf{b}\, dV + \int_S \mathbf{N}^T\,\mathbf{q}\, dS \tag{15}$$

For displacement-independent loads, the nonlinear equilibrium can be written as:

$$\mathbf{r}(\mathbf{u},\lambda) = \mathbf{g}(\mathbf{u}) - \mathbf{f} = \mathbf{g}(\mathbf{u}) - \lambda\,\mathbf{q} \tag{16}$$

where $\boldsymbol{q}$ is a reference load vector and λ is the load factor. The equation is solved in each step for $\boldsymbol{r} = 0$ using an appropriate path-following method, such as the Load Control, Displacements Control, or the Arc-Length Method, which are based on Newton-Raphson method iterations.

The nonlinear problem can be solved by an incremental and iterative approach, such as the Newton-Raphson method. In each step, for a given displacement $\boldsymbol{u}_e$, the stiffness matrix is given by the differentiation of the internal forces vector:

$$\mathbf{K}_T = \frac{\partial \mathbf{G}}{\partial \boldsymbol{u}} = \mathbf{K}_L + \mathbf{K}_\sigma \tag{17}$$

where the material stiffness matrix $\mathbf{K}_L$ and the geometric stiffness matrix $\mathbf{K}_\sigma$ are given by:

$$\mathbf{K}_L = \int_V \overline{\mathbf{B}}^T \frac{\partial \hat{\boldsymbol{\sigma}}}{\partial \mathbf{u}_e}\, dV = \int_V \overline{\mathbf{B}}^T\,\mathbf{C}\,\overline{\mathbf{B}}\, dV, \qquad \mathbf{K}_\sigma = \int_V \frac{\partial \overline{\mathbf{B}}^T}{\partial \mathbf{u}_e} \boldsymbol{\sigma}\, dV = \int_V \mathbf{G}^T\,\mathbf{S}\,\mathbf{G}\, dV \tag{18}$$

where $\mathbf{C}$ is the constitutive matrix, presented in Eq. (7) for FG composites, and:

$$\overline{\mathbf{B}} = \mathbf{B}_0 + \mathbf{B}_L, \quad \mathbf{S} = \begin{bmatrix} \overline{\mathbf{S}} & 0 & 0 \\ 0 & \overline{\mathbf{S}} & 0 \\ 0 & 0 & \overline{\mathbf{S}} \end{bmatrix}, \quad \overline{\mathbf{S}} = \begin{bmatrix} \sigma_x & \tau_{xy} & \tau_{xz} \\ \tau_{xy} & \sigma_y & \tau_{yz} \\ \tau_{xz} & \tau_{yz} & \sigma_z \end{bmatrix} \tag{19}$$

For a more efficient implementation, instead of computing the integral in the entire volume, we perform the Gaussian integration in the isogeometric element, defined by the knot spans in the three parametric directions. This is similar to what is performed in FEM for the assembly of the global stiffness matrix.

3 Numerical examples

In order to verify the isogeometric formulation presented in this work, a 2-D benchmark proposed by Paulino and Kim [5] was considered. This example considers a two-dimensional FGM structure simply supported in left edge and subjected to a uniform tension load of unit value at the right edge, as illustrated by Fig. 1. The structure has unit thickness and the modulus of elasticity variation in the vertical (y) direction is given by:

$$E(y) = E_0\, e^{\beta(2-y)} \tag{20}$$

where $E_0 = 1$ and $\beta = \log(4)/2$. Therefore, $E(0) = 4$ GPa and $E(2) = 1$ GPa. This variation was simulated in the numerical solution using the Rule of Mixtures for a fictitious FGM with $E_m = 0$, $E_c = 4$, and $V_c = E(y)/E_c$, resulting in an exponential variation of the volume fraction with $V_c(0) = 1$ and $V_c(2) = 0.25$. The volume fractions at control points are computed using a equally spaced sample points in parameter space.

The isogeometric mesh is refined by both h and p-refinement methods, in order to study the convergence of the proposed formulation. The results are presented in Table 1, while some of the distinct mesh utilized are shown in Fig. 2. It is important to highlight that, due to the boundary conditions, when using the p-refinement, the intermediate control point on the left edge must be interpolated by the shape functions in order to guarantee the prescribed displacement. Thus, its multiplicity must be increased along with the NURBS degree.

As can be seen in Table 1, by using a h-refinement approach, the isogeometric results converge to the analytical results, evidencing the implementation consistency. The same behavior is observed when using the p-refinement, once higher-degree NURBS return closer displacements to the analytical solution for the same number of elements. Additionally, it is important to highlight that the p-refinement provides a higher convergence rate, as the 8 x 4 cubic elements mesh leads to almost exact displacements.

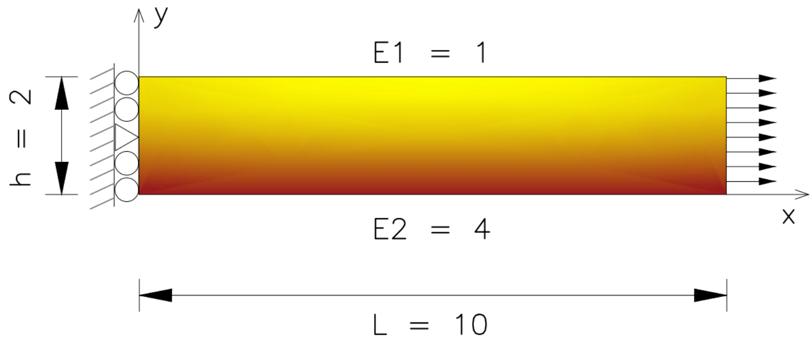

Figure 1. Functionally Graded 2D-structure.

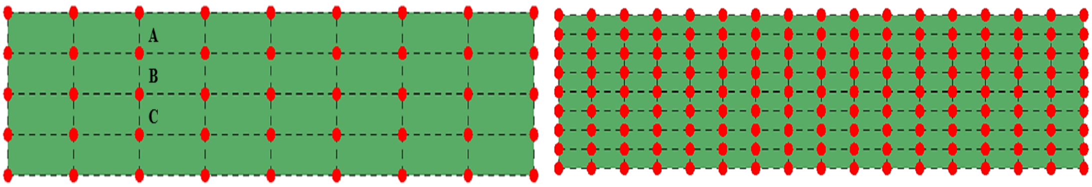

(a) 8x4 isogeometric linear mesh.

(b) 16x8 isogeometric linear mesh.

Figure 2. Mesh obtained by h-refinement.

Table 1. Nodal displacements for distinct mesh refinements.

Displ.	8 x 4			16 x 8			Analytical [5]
	Linear	Quadratic	Cubic	Linear	Quadratic	Cubic	
u_A	0.9884	1.0854	1.1590	1.1110	1.1351	1.1589	1.1585
v_A	1.6649	1.7198	1.7723	1.7425	1.7566	1.7723	1.7720
u_B	0.8999	0.9941	1.0653	1.0189	1.0417	1.0653	1.0650
v_B	1.3049	1.3222	1.3461	1.3349	1.3391	1.3461	1.3460
u_C	0.8330	0.9267	0.9974	0.9512	0.9731	0.9973	0.9970
v_C	0.9450	0.9245	0.9200	0.9273	0.9206	0.9200	0.9200

Once the model is validated, another numerical example can be simulated. A Functionally Graded cantilever beam is subjected to a load at the tip. It has a circular cross-section and the volume fraction variation now occurs in the x-axis direction, being defined by:

$$V_c = 1 - \left(\frac{x}{L}\right)^N \tag{21}$$

where N is a user-controlled factor that allows the employment of multiple profiles. The effective properties throughout the gradation are evaluated by the Rule of Mixtures, with $E_c = 380$ GPa and $E_m = 90$ GPa, as seen in Fig. 3. For this example, $P = 40$ kN, $L = 10$ m, $r = 0.728$ m, and $N = 1$.

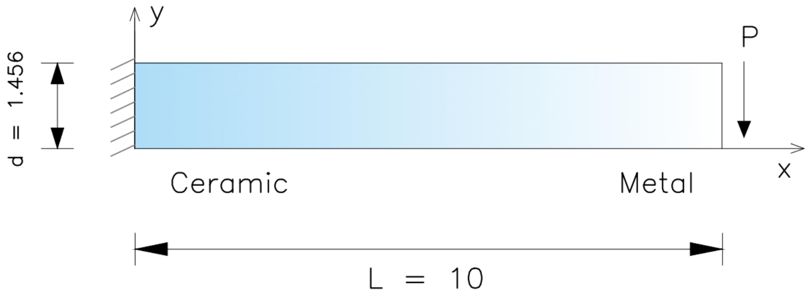

Figure 3. Functionally Graded Beam.

A reference solution can be obtained by the unit load method (ULM), as the structure is statically determinate. In order to provide a higher quality evaluation, the shear contribution is considered. The tip displacement of a cantilever beam is given by:

$$w_{max} = \int_L \frac{\overline{M}M}{EI}dx + \int_L f_s\frac{\overline{Q}Q}{GA}dx = \int_0^L \frac{P(L-x)^2}{E(x)I}dx + \int_0^L f_s\frac{P}{G(x)A}dx \tag{22}$$

The structure is modelled as a 3D-solid. Once the p-refinement presented a higher convergence-rate, it was the sole method utilized to refine the discretization. The initial isogeometric mesh contains 8 x 4 x 4 elements, with a higher discretization along the gradation direction. Additionally, it is important to note that, as the cross-section presents a circular geometry, the shape functions are required to be at least quadratic within their plane. Thus, the initial NURBS degree is 2. The results are shown in Table 2, whilst the mesh and the deformed configuration can be seen in Fig. 4.

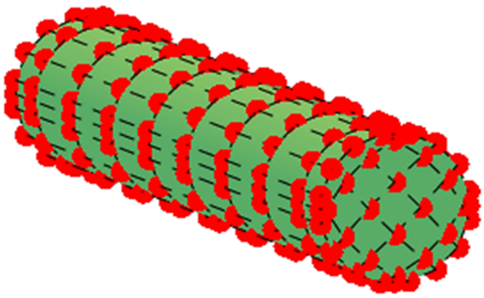

(a) 8 x 4 x 4 isogeometric quadratic mesh.

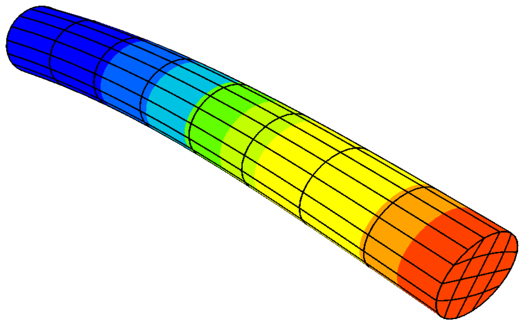

(b) Structure deformed configuration.

Figure 4. Isogeometric analysis of FG beam.

Table 2. FG cantilever beam tip transversal displacement.

Material	8 x 4 x 4		ULM (mm)	Diff. (Quad.)	Diff. (Cubic)
	Quadratic	Cubic			
Ceramic	0.1579	0.1588	0.1591	-0.70%	-0.17%
FGM	0.2058	0.2068	0.2081	-1.09%	-0.66%
Metal	0.6668	0.6704	0.6716	-0.70%	-0.17%

As seen in Table 2, the results are very close, differing by fewer than 1% for both isotropic and FGM. The ULM uses 1-D beam theory assumptions, hence the difference due to distinct kinematic hypothesis considerations between the ULM and the full 3D model.

In terms of the mesh refinement and convergence process, the degree elevation of the used shape functions provided a small accuracy enhancement, showing that the original mesh already provides a good approximation. Additionally, the FGM results present a higher difference when compared to the proposed solution than the homogeneous. This is expected, once the effective properties variation makes FG structures require finer discretizations.

The structure behavior considering the geometric nonlinearity is also studied. By increasing the applied load, the displacements initially increase along in a linear rate. Although, when a large enough displacement is reached, the structural response behavior is altered, with the behavior becoming nonlinear.

In order to validate the nonlinear implementation, the displacements of a ceramic beam are compared with results obtained using the *Elastica* solution through elliptic integrals [6]. Both axial and transversal displacements are considered. The variables are measured in terms of dimensionless parameters, given respectively for load and displacements by PL^2/E_cI and $v, u/L$. The load-displacements curves for the ceramic, metallic, and FGM beams are shown in Fig. 5.

These results show the ceramic nonlinear response is almost coincident with the reference solution. Once it simulates the stiffest structure, the ceramic homogeneous beam returns the lowest displacements for any given load. On the other hand, the metallic homogeneous beam is the most flexible, returning the highest displacements for any given load. The FGM structure, as a composite made by distinct volume fractions from both materials, presents an intermediate load-displacement path, assuring the consistency of the nonlinear implementation.

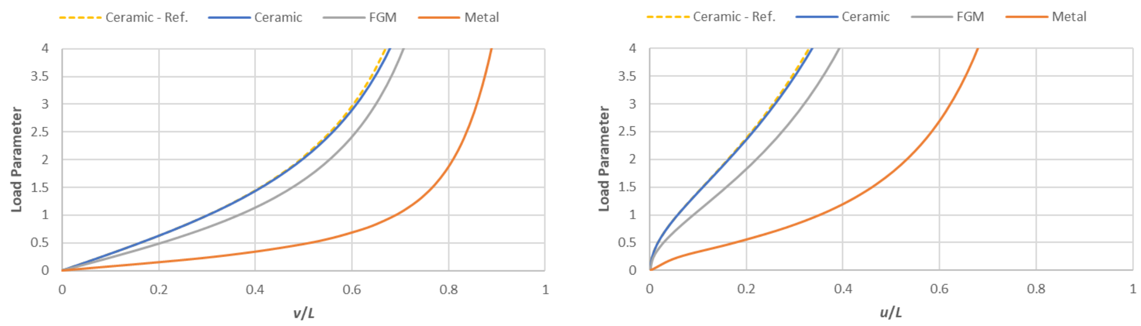

(a) Transversal displacement.

(b) Axial displacement.

Figure 5. Load-displacement curves.

Finally, the geometric nonlinearity is important only for very large transversal displacements. For example, when considering the FGM, the load-displacement curve is almost linear for values up to 35%-40% of the length. On the other hand, for the axial displacements, the nonlinearity assumptions becomes relevant to the analysis much sooner.

4 Conclusion

This work present a NURBS-based isogeometric approach to geometrically nonlinear analysis of 3D FGM structures. In this formulation, the volume fraction variation within the structure is described using the same basis functions adopted to geometry description and displacement approximation. This approach allows the analysis of 3D structures with arbitrary geometry and material gradation. Furthermore, model refinement can be easily performed using the classical geometric modeling algorithms of knot insertion and degree elevation.

The results showed that the formulation and implementation presented in this work is valid, once it provided outputs close to the reference values found in the literature for linear and geometrically nonlinear analysis considering different geometries and gradation profiles. Both h- and p-refinements were successfully used, but the results showed that using higher order basis functions leads to faster convergence, requiring fewer degrees of freedom in comparison to lower order functions.

Acknowledgements. The authors gratefully acknowledge CNPq (Conselho Nacional de Desenvolvimento Científico e Tecnológico) and FUNCAP (Fundação Cearense de Apoio ao Desenvolvimento Científico e Tecnológico) for the financial support.

Authorship statement. The authors hereby confirm that they are the sole liable persons responsible for the authorship of this work, and that all material that has been herein included as part of the present paper is either the property (and authorship) of the authors, or has the permission of the owners to be included here.

References

[1] H. S. Shen. *Functionally graded materials: Nonlinear analysis of plates and shells*. CRC Press, 2009.

[2] T. J. R. Hughes, J. A. Cotrell, and Y. Bazilevs. Isogeometric analysis: Cad, finite elements, nurbs, exact geometry and mesh refinement. *Computer Methods in Applied Mechanics and Engineering*, vol. 194, pp. 4135–4195, 2005.

[3] J. H. Kim and G. H. Paulino. Isoparametric graded finite elements for nonhomogeneous isotropic and orthotropic materials. *Journal of Applied Mechanics*, vol. 69, n. 4, pp. 502–514, 2002.

[4] A. H. Akbarzadeh, A. Abedini, and Z. T. Chen. Effect of micromechanical models on structural responses of functionally graded plates. *Composite Structures*, vol. 119, pp. 598–609, 2015.

[5] J. H. Kim and G. H. Paulino. The weak patch test for nonhomogeneous materials modeled with graded finite elements. *Journal of the Brazilian Society of Mechanical Sciences and Engineering*, vol. 29, pp. 63–81, 2007.

[6] K. Mattiasson. Numerical results from large deflection beam and frame problems analyzed by means of elliptic integrals. *International Journal for Numerical Methods in Engineering*, vol. 17, pp. 145 – 153, 1981.